

Compositional Control of Higher Order Assembly Using Synthetic Collagen Peptides

Fei Xu,[†] Ji Li,[‡] Vikas Jain,[§] Raymond S. Tu,[§] Qingrong Huang,[‡] and Vikas Nanda*,[†]

[†]Department of Biochemistry, Robert Wood Johnson Medical School, UMDNJ and the Center for Advanced Biotechnology and Medicine, Piscataway, New Jersey 08854, United States

[‡]Department of Food Science, Rutgers, the State University of New Jersey, 65 Dudley Road, New Brunswick, New Jersey 08901, United States

[§]Department of Chemical Engineering, The City College of City University of New York, 140th Street and Convent Avenue, Steinman Hall T313, New York, New York 10031, United States

S Supporting Information

ABSTRACT: We present the case of a two-component collagen peptide hydrogel that self-assembles through non-covalent electrostatic interactions. Natural collagen materials, such as those of connective tissue or the basement membrane, assemble in a hierachic fashion. Similarly, the synthetic peptides presented here proceed from monomer to trimer to fiber and, finally, to a hydrogel. By varying stoichiometry and concentration, we are able to dissect the stages of higher order assembly. Insight gained from this study will improve the molecular design of biomimetic materials.

Collagen has many favorable properties making it an attractive target for biomaterials: low antigenicity, biodegradability, low toxicity, and high biocompatibility.^{1,2} Currently, animal-derived collagens are utilized in biomedical, cosmetic, and food science applications, but they are costly to purify and run the risk of prion contamination.^{1,3} Synthetic collagens could circumvent some of these issues and potentially allow greater control of material properties.

α -Helical or β -hairpin peptides have been successfully designed to form self-assembling materials.⁴ Although natural collagens are widely used, only a few recent examples of designed collagen peptide materials exist.⁵ A greater diversity of available cross-linking elements will facilitate the design of complex functional biomaterials. Different molecular strategies, such as using side chain hydrophobic and electrostatic interactions, disulfide or metal mediated cross-linking, have successfully induced higher order assembly of collagen-like peptides.^{6–8} The assembled structures ranged from particles and fibers to sheets. Here, we use electrostatic interactions not only to drive fiber formation but also to further induce assembly of a hydrogel, a transparent, highly hydrated polymer network. Hydrogels are a useful phase of biomaterials that have clear applications in tissue regeneration and drug delivery.^{9,10}

We hypothesize that using heterotrimeric collagen peptides will allow control over the higher order assembly and chemical functionality of biomaterials. Recently, there has been significant progress in the design of heterotrimeric collagen peptides,¹¹ and disulfide cross-linking of neutral collagen peptides has been used to design heterotrimers that assemble

into fibrils.⁸ The two peptides described in this study use electrostatic interactions between acidic and basic amino acids to form heterotrimers that further associate. By varying peptide stoichiometry and total concentration, we are able to modulate the nature of higher order assembly.

In previous work, three Charged Peptides (referred herein as CPA, CPB, and CPC) were designed to form a mixture of heterotrimers.¹² Although it was found that a 2:1 ratio of CPB to CPC formed stable and soluble triple helices, a 1:2 mixture resulted in rapid aggregation at low temperatures. This discrepancy motivated us to explore the effects of composition on higher order assembly. Below, we demonstrate the complex dependence of assembly on concentration and mixing the stoichiometry of CPB and CPC.

The relationship between composition and assembly is best visualized using a phase diagram where the axes are peptide concentration (Figure 1). The relative mixing ratio of the two peptides divides the phase diagram into two domains. The

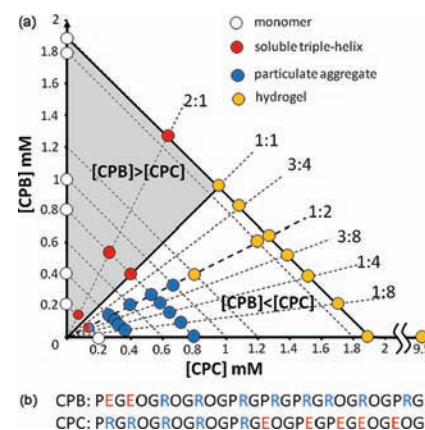


Figure 1. (a) Phase diagram of CPB and CPC combinations at 4 °C. Radial dashed lines constrain the peptide mixing ratio (annotated as CPB:CPC), while parallel lines constrain total peptide concentration. The domain where $[CPB] > [CPC]$ is represented as the (b) sequences of CPB and CPC. P = proline, R = arginine, E = glutamic acid, O = hydroxyproline.

Received: August 17, 2011

Published: December 13, 2011

upper domain where $[CPB] > [CPC]$ is characterized solely by soluble monomeric or triple-helical species. The lower domain where $[CPB] \leq [CPC]$ yields properties that are pertinent for materials development, and mixtures form various higher-order assemblies. In this domain, total concentration determines whether aggregates form an opaque precipitate or a semi-transparent hydrogel. The relative ratio of CPB:CPC influences aggregate morphology, which can range from particles to fibers. We explore the mechanisms of assembly in the lower domain of this phase diagram.

Previously we observed that a 0.2 mM CPB:2CPC mixture aggregated overnight.¹² Increasing the concentration above 0.3 mM significantly accelerates aggregation. By 0.8 mM, aggregation is essentially complete within 30 min (Figure 2a).

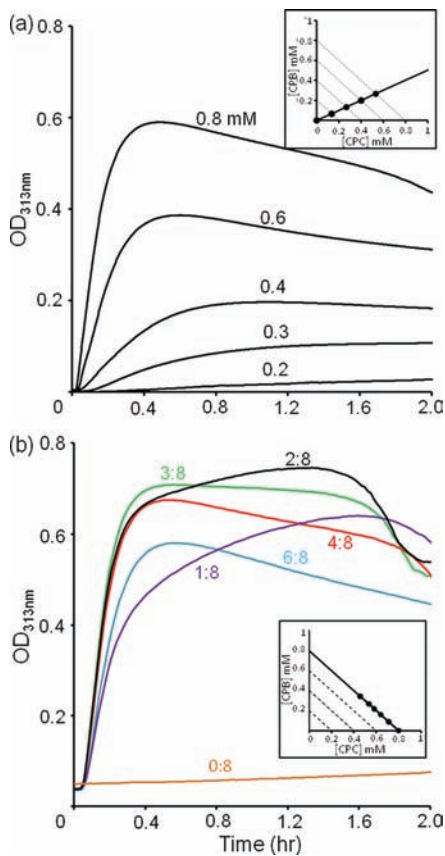


Figure 2. Turbidity kinetics at 4 °C of (a) CPB:2CPC for total concentration from 0.2 to 0.8 mM (b) CPB:CPC with various mixing ratios at a total concentration 0.8 mM.

The subsequent drop of signal is presumably due to settling of the precipitate.

The relative fraction of CPB and CPC in the mixture also has a significant impact on the rate of aggregation. Assemblies are monitored for a series of mixing ratios, holding the total concentration at 0.8 mM (Figure 2b). CPC alone requires 2–3 days to form a visible precipitate. Aggregation is most efficient at 3:8. This is surprising because one would expect the optimal ratio for collagen peptide assembly to be consistent with formation of a trimeric species, i.e. 3:0, 1:2, 2:1, or 0:3. The increase of turbidity correlates with an increase in particle size as measured by multiangle static light scattering (Figure S1). Again the particle size increases most rapidly at mixing ratio 3:8 even though the concentration is lower (0.1 mM). As these are

kinetics experiments, it is necessary to explore whether these properties are relevant in the equilibrium composition of peptide aggregates.

The observed noncanonical 3:8 mixing ratio raises the question whether CPB is physically part of the aggregate or is somehow serving a catalytic role in nucleating assembly. To determine this, the peptide content of precipitates is determined by HPLC for several initial mixing ratios at 0.8 mM. Peptide CPB is found in the precipitate indicating that it was in fact physically part of the aggregate. When the starting ratio of CPB to CPC was 1:8, or 1:4, the resulting ratio of peptides in the precipitate matches the starting ratio (Table 1). However, as the

Table 1. Initial Mixing Ratio vs Compositional Ratio of Aggregates of CPB:CPC Obtained by HPLC^a

Initial Mixing Ratios	Composition ratios of aggregates
1:8	1.32 ± 0.13:8
2:8	2.00 ± 0.13:8
3:8	2.29 ± 0.33:8
4:8	2.76 ± 0.18:8
6:8	3.10 ± 0.07:8

^aPeak areas of CPB and CPC were used to obtain final ratios. Final composition deviates significantly from the initial conditions for mixing ratios at 3:8 or above.

relative amount of CPB increased, we observe a limiting compositional ratio of ~3:8. This unusual property suggests that composition may be influenced by long-range interactions at the level of higher order assembly rather than triple helix formation.

If long-range forces, presumably electrostatics, are responsible for mediating assembly, then screening charged side chain interactions would prevent aggregation. As the salt concentration was increased, the aggregation rate and total extent of aggregate were reduced (Figure 3).

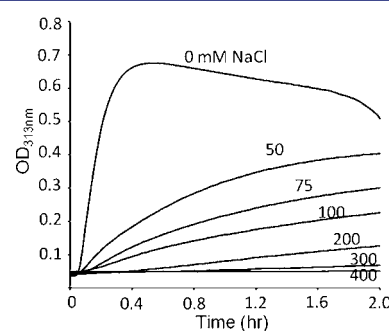


Figure 3. Salt effects on the turbidity of mixture 1CPB:2CPC at the total concentration 0.8 mM. Turbidity was monitored at 4 °C.

Although it was previously determined that mixtures of CPB and CPC formed triple helices, the 3:8 composition of the aggregate calls into question whether secondary structure is

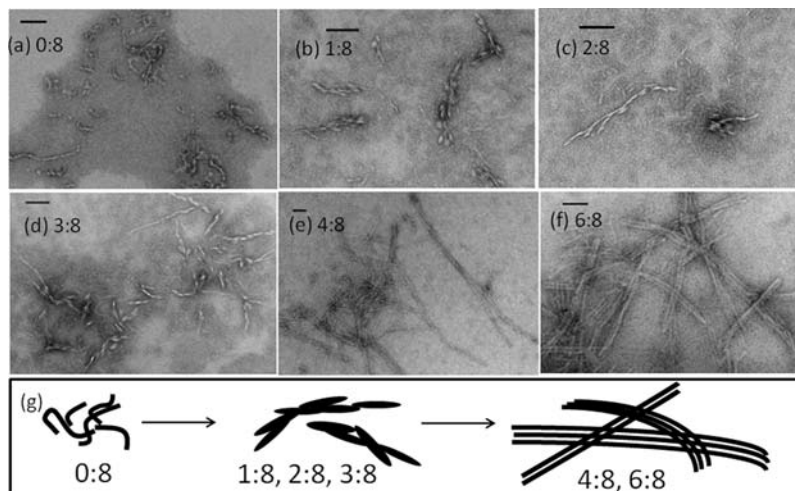


Figure 4. Electron microscopy images of negatively stained CPB:CPC samples at various mixing ratios (a) 0:8, (b) 1:8, (c) 2:8, (d) 3:8, (e) 4:8, and (f) 6:8 in pH 7, 10 mM phosphate buffer. (g) Schematic sketch of fiber morphology under various mixing ratio. The scale bar is 100 nm. Except for CPC alone or 0:8 at 0.8 mM, all the samples were prepared at the same total concentration, 0.4 mM, and incubated at 4 °C for ~72 h.

required for higher order assembly. Perhaps the zwitterionic nature of CPC is sufficient to drive assembly through non-specific electrostatic interactions. The following two observations support a secondary structure prerequisite for assembly: (1) the rate and extent of aggregation decreases with increasing temperature and (2) directly inhibiting triple-helix formation by mutating core glycines prevents aggregation.

If the assembly of CPB and CPC requires a folded intermediate, then raising the temperature should denature the intermediate, preventing or slowing the rate of aggregation at a specific concentration. A 0.8 mM 1:2 mixture was rapidly cooled from a temperature well above the observed melting transition (Figure S2). Aggregation was most efficient at 4 °C. No aggregation was observed at 15 °C, even after several hours.

If aggregation is mediated by nonspecific electrostatic interactions, replacing CPC with a modified sequence that has a similar charge distribution but cannot form triple helices might still promote aggregation. To test this hypothesis, we synthesized CPC-G/P, in which all 10 glycines in CPC were replaced by prolines. A circular dichroism (CD) spectrum of CPC-G/P indicates a polyproline II random-coil state (Figure S3a) instead of a triple helix. A 1:2 mixture of CPB:CPC-G/P also lacked secondary structure as measured by CD. Small-angle X-ray scattering (SAXS) measurements are best fit with a circular cylinder model at the Guinier region to $\sim 15 \times 90$ Å for an individual rod of CPB:2CPC,¹³ which is reasonable for a 30 amino acid long triple helix (Figure S4d). Fitted SAXS data for CPB:2CPC-G/P are consistent with a random coil configuration (Figure S4). More importantly, mutating CPC prevented aggregation (Figure S3b). A triple-helical intermediate rather than an unfolded state is necessary for the formation of a higher-order structure.

Transmission Electron Microscopy (TEM) images of the CPB/CPC assemblies reveal a transition in aggregate morphology when the composition is 3:8 (Figure 4). CPC alone requires high concentrations to get reasonable aggregation densities for EM imaging and are observed to form curly, gnarled fibers. Addition of a small amount of CPB where CPB:CPC \leq 3:8 results in elongated, granular particles. In contrast, peptide compositions above 3:8 formed fibers of uniform thickness up to 1 μ m in length, often found in bundles where the individual fibers are clearly visible. Below 3:8, many

of the images show heterogeneous mixtures of structures, including the coexistence of granular particles and long, thin fibers. Above 3:8, the fiber morphologies are consistently observed in multiple preparations (Figure S5).

The thickness of individual fibers is uniformly ~ 12 nm, near the length of a 30-residue triple helix, suggesting that individual peptides may be aligned perpendicular to the fiber axis. The addition of two amino acids at the N-terminus of CPB did not disrupt aggregation or fiber morphology (Table S1 and Figure S6). In other synthetic peptides and some natural collagens, periodic banding along the fiber axis is caused by coherent gaps between adjacent chains.^{7,14} Such banding is not observed in this system and would not be expected if peptides are associating perpendicular to the fiber axis.

At concentrations >0.8 mM, CPB:2CPC mixtures are semi-transparent rather than opaque. Samples do not flow when the tube containing them is inverted, suggesting formation of a peptide hydrogel. This is confirmed using microrheological measurements. The trajectories of 1.0 μ m fluorescent polystyrene beads embedded in samples are videotaped and analyzed to determine the mean square displacement as a function of time.¹⁵ At total concentrations of <0.8 mM, the mixture behaves as a viscous solution where $G'' > G'$ at all frequencies (Figures 5 and S7). Above this concentration, G'

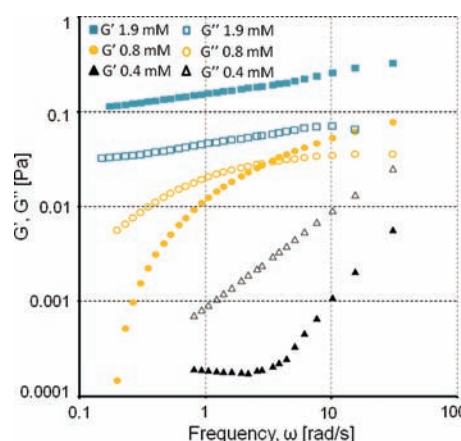


Figure 5. Storage and loss moduli G' and G'' of CPB:2CPC at 4 °C.

exceeds G", indicating formation of a soft hydrogel. CD of a 2 mM CPB:2CPC sample in a thin cuvette showed the presence of a collagen triple helix in the hydrogel (Figure S8). Although others have synthesized collagen peptide hydrogels using disulfide cross-linking, the peptide concentrations required for gelation are 10- to 20-fold higher (~10% vs 0.6% w/v).

It is possible to control the nature of the assembly and material properties of the two-component system by varying the mixing ratio and total concentration of the charged peptides. The advantage of the two-component system is the ability to generate a library of compositions with tunable material properties. We have only begun to characterize the rich behavior of these peptides, and there are still significant unexplored areas of this phase diagram that may present unique behaviors in terms of aggregate morphology or material rheology. Multicomponent systems might be used to generate spatial gradients within a material such as discrete or gradual changes in mechanical properties or the density of ligand functionalization. Such applications would require further optimization of material, perhaps by replacing arginine with lysine and glutamate with aspartate, thus forming more stable ion pairs,¹⁶ or by including structured hydrophobic domains¹⁰ that could improve the practical utility of this system.

The disconnect between the optimal peptide ratio for aggregation and the canonical stoichiometry of a collagen triple helix highlights a key challenge in the rational design of peptide biomaterials. The current design process is focused on optimizing atomic-scale interactions such as protein topology or intermolecular association. The ability of the assembling fiber to constrain the peptide composition to ~3 CPB:8 CPC suggests that long-range forces are playing a significant role in specifying the structure of the final assembly. We suspect that for ratios >3:8 the charge density of cationic CPB is too high to allow efficient aggregation, and >1:1 no higher-order assembly of any kind is observed. As such, the assembly is able to maintain the ratio of charged to neutral peptides. The repulsive interactions may also direct morphology by favoring a uniform fiber over granular particles.^{10,17} These types of interactions represented uncharted territory for computational protein design and will require the development of new multiscale computational methods that treat the structure of fibrous proteins atomistically and consider protein fibers as polyelectrolytes in higher order association processes.¹⁸

ASSOCIATED CONTENT

Supporting Information

Methods, data analysis, additional figures and tables. This material is available free of charge via the Internet at <http://pubs.acs.org>.

AUTHOR INFORMATION

Corresponding Author

nanda@cabm.rutgers.edu

ACKNOWLEDGMENTS

F.X., V.N.: NIH DP2 OD006478-01, NSF DMR-0907273. J.L., Q.H.: USDA National Research Initiative (#2009-35603-05071). R.T., V.J.: NSF DMR-1006407.

REFERENCES

- (1) Lee, C. H.; Singla, A.; Lee, Y. *Int. J. Pharm.* **2001**, *221*, 1.
- (2) Friess, W. *Eur. J. Pharm. Biopharm.* **1998**, *45*, 113. Rao, K. P. *J. Biomater. Sci.* **1995**, *7*, 623.
- (3) O'Grady, J. E.; Bordon, D. M. *Adv. Drug Delivery Rev.* **2003**, *55*, 1699.
- (4) Pandya, M. J.; Spooner, G. M.; Sunde, M.; Thorpe, J. R.; Rodger, A.; Woolfson, D. N. *Biochemistry* **2000**, *39*, 8728. Pochan, D. J.; Schneider, J. P.; Kretsinger, J.; Ozbas, B.; Rajagopal, K.; Haines, L. *J. Am. Chem. Soc.* **2003**, *125*, 11802.
- (5) O'Leary, L. E. R.; Fallas, J. A.; Bakota, E. L.; Kang, M. K.; Hartgerink, J. D. *Nat. Chem.* **2011**, *3*, 821.
- (6) Kar, K.; Ibrar, S.; Nanda, V.; Getz, T. M.; Kunapuli, S. P.; Brodsky, B. *Biochemistry* **2009**, *48*, 7959. Przybyla, D. E.; Chmielewski, J. *J. Am. Chem. Soc.* **2008**, *130*, 12610. Cejas, M. A.; Kinney, W. A.; Chen, C.; Leo, G. C.; Toung, B. A.; Vinter, J. G.; Joshi, P. P.; Maryanoff, B. E. *J. Am. Chem. Soc.* **2007**, *129*, 2202.
- (7) Rele, S.; Song, Y.; Apkarian, R. P.; Qu, Z.; Conticello, V. P.; Chaikof, E. L. *J. Am. Chem. Soc.* **2007**, *129*, 14780.
- (8) Kotch, F. W.; Raines, R. T. *Proc. Natl. Acad. Sci. U.S.A.* **2006**, *103*, 3028.
- (9) Petka, W. A.; Harden, J. L.; McGrath, K. P.; Wirtz, D.; Tirrell, D. A. *Science* **1998**, *281*, 389. Nagarkar, R. P.; Hule, R. A.; Pochan, D. J.; Schneider, J. P. *J. Am. Chem. Soc.* **2008**, *130*, 4466.
- (10) Nowak, A. P.; Breedveld, V.; Pakstis, L.; Ozbas, B.; Pine, D. J.; Pochan, D.; Deming, T. *J. Nature* **2002**, *417*, 424.
- (11) Gauba, V.; Hartgerink, J. D. *J. Am. Chem. Soc.* **2007**, *129*, 2683.
- (12) Xu, F.; Zhang, L.; Koder, R. L.; Nanda, V. *Biochemistry* **2010**, *49*, 2307.
- (13) Ilavsky, J.; Jemian, P. R. *J. App. Cryst.* **2009**, *42*, 347. Roe, R. J. *Methods of X-ray and Neutron Scattering in Polymer Sciences*; Oxford University Press: 2000.
- (14) Papapostolou, D.; Smith, A. M.; Atkins, E. D. T.; Oliver, S. J.; Ryadnov, M. G.; Serpell, L. C.; Woolfson, D. N. *Proc. Natl. Acad. Sci. U.S.A.* **2007**, *104*, 10853. Kadler, K. E.; Hojima, Y.; Prockop, D. J. *Biochem. J.* **1990**, *268*, 339.
- (15) Mason, T. G.; Weitz, D. A. *Phys. Rev. Lett.* **1995**, *74*, 1250. Zimenkov, Y.; Dublin, S. N.; Ni, R.; Tu, R. S.; Breedveld, V.; Apkarian, R. P.; Conticello, V. P. *J. Am. Chem. Soc.* **2006**, *128*, 6770.
- (16) Gauba, V.; Hartgerink, J. D. *J. Am. Chem. Soc.* **2007**, *129*, 15034.
- (17) Nowak, A. P.; Breedveld, V.; Pine, D. J.; Deming, T. *J. Am. Chem. Soc.* **2003**, *125*, 15666.
- (18) Dobrynin, A. V.; Rubinstein, M. *Prog. Polym. Sci.* **2005**, *30*, 1049.